Modelling of wave-induced non linear dynamic soil response in vertical breakwaters foundation

Une modélisation de la réponse dynamique non linéaire du sol de fondation de digues verticales induite par le mouvement des vagues.

Sitckle M.M., de la Fuente P.
Univ. Politécnica de Madrid, Spain

Oteo C.
Univ. da Coruña, Spain

ABSTRACT: A theoretical and numerical framework to model the soil-water-structure interaction involved in a breakwater structure subjected to sea wave actions, focused in the special case of impulsive sea wave actions due to breaking waves, is presented. The model includes i) soil skeleton-pore fluid interaction governed by the u-p_w Generalized Biot formulation including dynamic effects, ii) non-linear elastoplastic soil behaviour described by a Generalized Plasticity sand constitutive model coupled with a conservative hyperelastic formulation for the dependence of the elastic stiffness on the stress, iii) coupling between caisson an rubble mound through a non-linear frictional contact constraint model. The Finite element numerical solution of the settled governing equations is outlined. A large scale model test is numerically reproduced under the scope of the proposed soil-water-structure interaction model. The wave-induced soil response mechanisms experimentally observed have been numerically reproduced.

RÉSUMÉ : Un cadre théorique et numérique est présenté pour modéliser l'interaction sol-eau-structure dans le cas d'une digue verticale soumise aux actions des vagues dans le cas particulier d'actions dynamiques dues à des vagues déferlantes. Le modèle comprend, i) l'interaction squelette du sol- fluide interstitiel, gouvernée par la formulation u-p_w généralisée de Biot comprenant les effets dynamiques, ii) le comportement élastoplastique non-linéaire du sol décrit par un modèle constitutif de plasticité généralisée pour sables couplé avec une formulation conservative hyperélastique pour la dépendance du module élastique avec la contrainte, iii) couplage entre un caisson et un enrochement à l'aide d'un modèle non-linéaire de contact avec frottement. La solution numérique par éléments finis des équations correspondantes est décrite. Un essai à grande échelle est modélisé numériquement dans le cadre du modèle d'interaction sol-eau-structure proposé. Les mécanismes de réponse du sol aux sollicitations par les vagues observés expérimentalement sont bien reproduits par le modèle numérique.

KEYWORDS: soil-water-structure interaction, breakwater foundation, Generalized Biot, Generalized Plasticity, contact mechanics.

1 INTRODUCTION.

Caisson type breakwaters are one of the most commonly used marine structures. Unfortunately not enough attention has been devoted in the last century to geotechnical design aspects, as this was the case for the hydraulic and structural problems. On the other hand the damage suffered by many breakwaters has been related with wave induced foundation response. For example, under impact and cyclic wave loading, saturated soils may experience large unacceptable permanent deformations due to progressively drop of soil strength with a pore pressure build up (liquefaction).

Most of the developed researches (Yamamoto et al 1978, Jeng et al 2001) have modelled the seabed soil skeleton-pore fluid interaction through the pseudostatic Biot Formulation. This theory, even if it is the base of most of subsequence developments, does not include dynamic terms. However several researches (Jeng et al 2003, Ulker et al 2010) have shown the significant relation of these terms with the wave induced effective stress development.

Most soil models used in the investigations of sea floor dynamics have been limited to the poroelastic model. Only a few contributions (Pastor et al 2006) have incorporated advanced constitutive relations that are able to represent properly the features of soil response under cyclic loading. This is a prominent aspect within any model proposed to analyze the geomechanical behaviour of a breakwater foundation because is indispensable to investigate the possible degradation process, for example liquefaction, leading to a diffuse failure mechanism.

The caisson-rubble mound interaction phenomenon, responsible of the principal loads transmitted to the foundation, has been investigated mostly through elastic Mass-Spring-Dashpot models (Goda 1994, Oumeraci et al 1994) where the caisson structure is modelled as a point mass. These models are not able to analyze the different interface strain-stress states involved in this contact surface. Few researches have employed frictional contact mechanics of deformable bodies to represent this interaction phenomenon not analyzing geomechanical implication.

In the next chapter the proposed theoretical model for the soil-water-structure interaction involved in a breakwater structure subjected to sea wave actions is presented. Afterwards the Finite Element numerical solution is outlined leading to some related numerical analyses with reference to precise boundary value problems of specific physical nature in order to justify the theoretical model and its numerical approach.

2 SOIL-WATER-STRUCTURE THEORETICAL MODEL

The soil-water-breakwater interaction has been modelled coupling different physical systems, such that independent solution of each system being impossible without simultaneous solution of the others.

The physical systems involved in the soil-water-breakwater interaction analysis are the caisson, the rubble mound and the sea bed (Figure 1). The coupling among these three occurs on domain interface via the boundary conditions. The rubble mound and the sea bed are already coupled media, where skeleton-pore fluid interaction exists, and the coupling occurs through the governing partial differential equations describing each physical phase.

Sea waves are not modelled as a proper physical system in the proposed theoretical model, representing the sea wave actions exerted over the structure as boundary conditions.

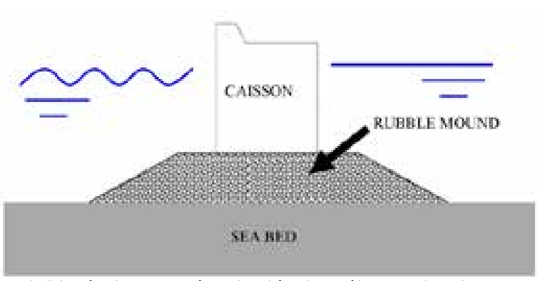

Figure 1. Physical systems involved in the soil-water-breakwater model

The theoretical model for the soil-water-breakwater interaction proposed is developed in two dimensions under plain strain idealization.

Once the sea bed, rubble mound and caisson governing equations are derived, including the couplings involved as well as the initial and boundary conditions, the theoretical model for the soil-water-breakwater interaction proposed will be set.

In following figure (Figure 2), the main parts of the theoretical model proposed in order to analyze the complex seafloor-rubble mound-caisson-swell interaction are schematically shown. The novel theoretical contributions appear in this figure over a dark colour box.

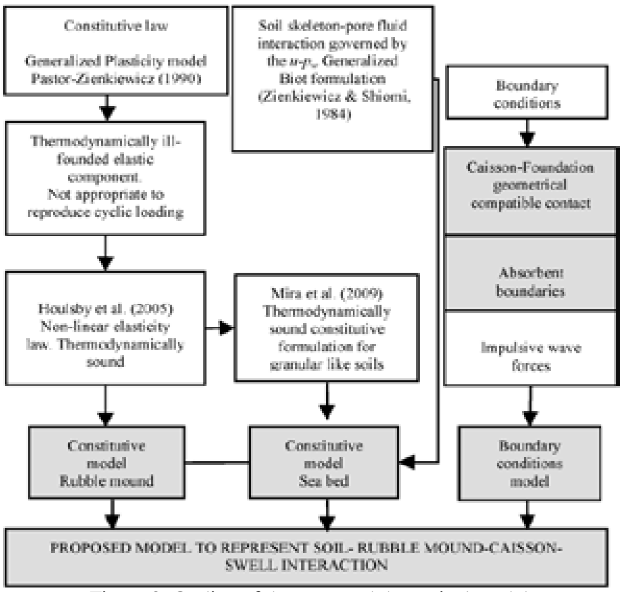

Figure 2. Outline of the proposed theoretical model

3 FINITE ELEMENT APROXIMATION

Once the kinematic relations as well as the constitutive laws are integrated in the balance equations, a system of five partial differential equations with five field variables is established. The field variables involved are: sea bed skeleton displacement $\boldsymbol{u}^{sb}$ and pore water pressure p_w^{sb}, rubble mound skeleton displacement $\boldsymbol{u}^{rm}$ and pore water pressure p_w^{rm} and caisson displacement $\boldsymbol{u}^{ca}$. The system of partial differential equations can be discretized using standard Galerkin techniques (Zienkiewicz et al 1999). After spatial discretization of the field variables, $\boldsymbol{u}^{sb} \cong \boldsymbol{N}^u \bar{\boldsymbol{u}}^{sb}$, $p_w^{sb} \cong \boldsymbol{N}^p \bar{\boldsymbol{p}}_w^{sb}$, $\boldsymbol{u}^{rm} \cong \boldsymbol{N}^u \bar{\boldsymbol{u}}^{rm}$, $p_w^{rm} \cong \boldsymbol{N}^p \bar{\boldsymbol{p}}_w^{rm}$, $\boldsymbol{u}^{ca} \cong \boldsymbol{N}^u \bar{\boldsymbol{u}}^{ca}$, the second order ordinary differential equation system (1)-(3) is obtained (Stickle 2010)

$$\boldsymbol{M}^{sb}\ddot{\bar{\boldsymbol{u}}}^{sb} + \boldsymbol{C}^{sb}\dot{\bar{\boldsymbol{u}}}^{sb} + \int_{\Omega^{sb}} \boldsymbol{B}^{\mathrm{T}}\boldsymbol{\sigma}'^{sb} d\Omega^{sb} - \boldsymbol{Q}^{sb}\bar{\boldsymbol{p}}_w^{sb} - \boldsymbol{f}^{sb1} = \boldsymbol{0} \quad (1)$$

$$\left(\boldsymbol{Q}^{sb}\right)^{\mathrm{T}} \dot{\bar{\boldsymbol{u}}}^{sb} + \boldsymbol{H}^{sb}\bar{\boldsymbol{p}}_w^{sb} + \boldsymbol{S}^{sb}\dot{\bar{\boldsymbol{p}}}_w^{sb} - \boldsymbol{f}^{sb2} = \boldsymbol{0}$$

$$\boldsymbol{M}^{rm}\ddot{\bar{\boldsymbol{u}}}^{rm} + \boldsymbol{C}^{rm}\dot{\bar{\boldsymbol{u}}}^{rm} + \int_{\Omega^{rm}} \boldsymbol{B}^{\mathrm{T}}\boldsymbol{\sigma}'^{rm} d\Omega^{rm} - \boldsymbol{Q}^{rm}\bar{\boldsymbol{p}}_w^{rm} - \boldsymbol{f}^{rm1} = \boldsymbol{0} \quad (2)$$

$$\left(\boldsymbol{Q}^{rm}\right)^{\mathrm{T}} \dot{\bar{\boldsymbol{u}}}^{rm} + \boldsymbol{H}^{rm}\bar{\boldsymbol{p}}_w^{rm} + \boldsymbol{S}^{rm}\dot{\bar{\boldsymbol{p}}}_w^{rm} - \boldsymbol{f}^{rm2} = \boldsymbol{0}$$

$$\boldsymbol{M}^{ca}\ddot{\bar{\boldsymbol{u}}}^{ca} + \boldsymbol{C}^{ca}\dot{\bar{\boldsymbol{u}}}^{ca} + \boldsymbol{K}^{ca}\bar{\boldsymbol{u}}^{ca} - \boldsymbol{f}^{ca} = \boldsymbol{0} \quad (3)$$

Where $\boldsymbol{B} = \boldsymbol{S}\boldsymbol{N}^u$ and

$$\boldsymbol{f}^{sb1} = \int_{\Omega^{sb}} \left(\boldsymbol{N}^u\right)^{\mathrm{T}} \rho^{sb}\boldsymbol{b}\, d\Omega^{sb} + \int_{\Gamma_t^{sb}} \left(\mathbf{N}^u\right)^{\mathrm{T}} \boldsymbol{t}_{imp}^{sb} d\Gamma_{\mathbf{t}}^{sb} + \mathbb{C}_r^{sb}$$

$$\mathbb{C}_r^{sb} = \left(\boldsymbol{R}_1 + \boldsymbol{R}_2 + \boldsymbol{R}_3\right)\dot{\bar{\boldsymbol{u}}}^{sb} \quad (4)$$

$$\boldsymbol{f}^{sb2} = \int_{\Omega^{sb}} \left(\nabla\boldsymbol{N}^p\right)^{\mathrm{T}} \mathbf{k}^{sb}\rho_w^{sb}\boldsymbol{b}\, d\Omega^{sb} + \int_{\Gamma_{p_w}^{sb}} \left(\boldsymbol{N}^p\right)^{\mathrm{T}} \boldsymbol{q}_{imp}^{sb} d\Gamma_{p_w}^{sb}$$

$$\boldsymbol{f}^{rm1} = \int_{\Omega^{rm}} \left(\boldsymbol{N}^u\right)^{\mathrm{T}} \rho^{rm}\boldsymbol{b}\, d\Omega^{rm} + \int_{\Gamma_t^{rm}} \left(\boldsymbol{N}^u\right)^{\mathrm{T}} \boldsymbol{t}_{imp}^{rm} d\Gamma_{\mathbf{t}}^{rm} + \mathbb{C}_c^{rm} \quad (5)$$

$$\boldsymbol{f}^{rm2} = \int_{\Omega^{rm}} \left(\nabla\boldsymbol{N}^p\right)^{\mathrm{T}} \mathbf{k}^{rm}\rho_w^{rm}\boldsymbol{b}\, d\Omega^{rm} + \int_{\Gamma_{p_w}^{rm}} \left(\boldsymbol{N}^p\right)^{\mathrm{T}} \boldsymbol{q}_{imp}^{rm} d\Gamma_{p_w}^{rm}$$

$$\boldsymbol{f}^{ca} = \int_{\Omega^{ca}} \left(\boldsymbol{N}^u\right)^{\mathrm{T}} \rho^{ca}\boldsymbol{b}\, d\Omega^{ca} + \int_{\Gamma_t^{ca}} \left(\boldsymbol{N}^u\right)^{\mathrm{T}} \boldsymbol{t}_{imp}^{ca} d\Gamma_{\mathbf{t}}^{ca} + \mathbb{C}_c^{ca} \quad (6)$$

The matrices given in the system (1)-(3) are defined by

$$\boldsymbol{M}^{sb} = \int_{\Omega^{sb}} \left(\boldsymbol{N}^u\right)^{\mathrm{T}} \rho^{sb}\boldsymbol{N}^u d\Omega^{sb}$$

$$\boldsymbol{M}^{rm} = \int_{\Omega^{rm}} \left(\boldsymbol{N}^u\right)^{\mathrm{T}} \rho^{rm}\boldsymbol{N}^u d\Omega^{rm} \quad (7)$$

$$\boldsymbol{M}^{ca} = \int_{\Omega^{ca}} \left(\boldsymbol{N}^u\right)^{\mathrm{T}} \rho^{ca}\boldsymbol{N}^u d\Omega^{ca}$$

$$\boldsymbol{Q}^{sb} = \int_{\Omega^{sb}} \boldsymbol{B}^{\mathrm{T}}\boldsymbol{m}\boldsymbol{N}^p d\Omega^{sb}\ , \boldsymbol{Q}^{rm} = \int_{\Omega^{rm}} \boldsymbol{B}^{\mathrm{T}}\boldsymbol{m}\boldsymbol{N}^p d\Omega^{rm} \quad (8)$$

$$\boldsymbol{S}^{sb} = \int_{\Omega^{sb}} \left(\boldsymbol{N}^p\right)^{\mathrm{T}} \frac{1}{Q^{sb}} \left(\boldsymbol{N}^p\right) d\Omega^{sb}$$

$$\boldsymbol{S}^{rm} = \int_{\Omega^{rm}} \left(\boldsymbol{N}^p\right)^{\mathrm{T}} \frac{1}{Q^{rm}} \left(\boldsymbol{N}^p\right) d\Omega^{rm} \quad (9)$$

$$\boldsymbol{H}^{sb} = \int_{\Omega^{sb}} \left(\nabla\boldsymbol{N}^p\right)^{\mathrm{T}} \frac{\mathbf{k}^{sb}}{\rho_w \cdot g} \left(\nabla\boldsymbol{N}^p\right) d\Omega^{sb}$$

$$\boldsymbol{H}^{rm} = \int_{\Omega^{rm}} \left(\nabla\boldsymbol{N}^p\right)^{\mathrm{T}} \frac{\mathbf{k}^{rm}}{\rho_w \cdot g} \left(\nabla\boldsymbol{N}^p\right) d\Omega^{rm} \quad (10)$$

$$\boldsymbol{C}^{sb} = \alpha^{sb}\boldsymbol{M}^{sb} + \beta^{sb}\boldsymbol{K}^{sb}$$

$$\boldsymbol{C}^{rm} = \alpha^{rm}\boldsymbol{M}^{rm} + \beta^{rm}\boldsymbol{K}^{rm} \quad (11)$$

$$\boldsymbol{C}^{ca} = \alpha^{ca}\boldsymbol{M}^{ca} + \beta^{ca}\boldsymbol{K}^{ca}$$

$$\boldsymbol{K}^{sb} = \int_{\Omega^{sb}} \boldsymbol{B}^{\mathrm{T}} \mathbf{D}^{sb}\left(\boldsymbol{\sigma}'^{sb}\right) \boldsymbol{B} \mathrm{d}\Omega^{sb}$$
$$\boldsymbol{K}^{rm} = \int_{\Omega^{rm}} \boldsymbol{B}^{\mathrm{T}} \mathbf{D}^{rm}\left(\boldsymbol{\sigma}'^{rm}\right) \boldsymbol{B} \mathrm{d}\Omega^{rm} \qquad (12)$$
$$\boldsymbol{K}^{ca} = \int_{\Omega^{ca}} \boldsymbol{B}^{\mathrm{T}} \mathbf{D}^{ca} \boldsymbol{B} \mathrm{d}\Omega^{ca}$$

The $\mathbf{C}_r^{sb}$ term in (4) represents the contribution of the radiation boundaries to the discretized governing equations, while $\mathbf{C}_c^{rm}$ and $\mathbf{C}_c^{ca}$ terms, appearing in (5) and (6), respectively, represents the contribution of the rubble mound - caisson contact to the discretized governing equations.

The proper choice of the element type in order to discretize the computational domain is of paramount importance as some elements introduce errors leading to unrealistic limit loads and spurious failure elements (Sloan et al 1982). Under Babuska-Brezzi robustness condition, keeping in mind the need of a C^0 interpolation for each field variable, in the present paper a mixed isoparametric lagrangian triangular element has been used, with 6 nodes quadratic interpolation for any skeleton displacement, $\boldsymbol{u}^{sb}$, $\boldsymbol{u}^{rm}$ and $\boldsymbol{u}^{ca}$, and 3 node linear interpolation for pore water pressure interpolation, p_w^{sb}, p_w^{rm}.

Temporal discretization of the displacements $\overline{\boldsymbol{u}}^{global} = \left[\overline{\boldsymbol{u}}^{sb}, \ \overline{\boldsymbol{u}}^{rm}, \ \overline{\boldsymbol{u}}^{ca}\right]^{\mathrm{T}}$ is performed by the Generalized Newmark *GN22* scheme while the excess pore pressure of the sea bed and rubble mound $\overline{\boldsymbol{p}}_w^{global} = \left[\overline{\boldsymbol{p}}_w^{sb}, \ \overline{\boldsymbol{p}}_w^{rm}\right]^{\mathrm{T}}$ are discretized by the *GN11* scheme, leading to the following difference equation

$$\begin{aligned}
\ddot{\overline{\boldsymbol{u}}}_{n+1}^{global} &= \ddot{\overline{\boldsymbol{u}}}_{n}^{global} + \Delta\ddot{\overline{\boldsymbol{u}}}_{n}^{global} \\
\dot{\overline{\boldsymbol{u}}}_{n+1}^{global} &= \dot{\overline{\boldsymbol{u}}}_{n}^{global} + \Delta t \cdot \ddot{\overline{\boldsymbol{u}}}_{n}^{global} + \beta_1 \cdot \Delta t \cdot \Delta\ddot{\overline{\boldsymbol{u}}}_{n}^{global} \qquad (13) \\
\overline{\boldsymbol{u}}_{n+1}^{global} &= \overline{\boldsymbol{u}}_{n}^{global} + \Delta t \cdot \dot{\overline{\boldsymbol{u}}}_{n}^{global} + \frac{1}{2}\Delta t^2 \cdot \Delta\ddot{\overline{\boldsymbol{u}}}_{n}^{global} + \frac{1}{2}\Delta t^2 \cdot \beta_2 \cdot \Delta\ddot{\overline{\boldsymbol{u}}}_{n}^{global}
\end{aligned}$$

$$\begin{aligned}
\dot{\overline{\boldsymbol{p}}}_{wn+1}^{global} &= \dot{\overline{\boldsymbol{p}}}_{wn}^{global} + \Delta\dot{\overline{\boldsymbol{p}}}_{wn}^{global} \qquad (14) \\
\overline{\boldsymbol{p}}_{wn+1}^{global} &= \overline{\boldsymbol{p}}_{wn}^{global} + \Delta t \cdot \dot{\overline{\boldsymbol{p}}}_{wn}^{global} + \Delta t \cdot \overline{\beta}_1 \cdot \Delta\dot{\overline{\boldsymbol{p}}}_{wn}^{global}
\end{aligned}$$

After the incorporation of difference equation (13) and (14) in (1)-(3) a non linear algebraic system is obtained where the unknown values are $\left[\Delta\ddot{\overline{\boldsymbol{u}}}_n^{sb}, \Delta\dot{\overline{\boldsymbol{p}}}_{wn}^{sb}, \Delta\ddot{\overline{\boldsymbol{u}}}_n^{rm}, \Delta\dot{\overline{\boldsymbol{p}}}_{wn}^{rm}, \Delta\ddot{\overline{\boldsymbol{u}}}_n^{ca}\right]$. The Newton-Raphson scheme is used to solved the non linear algebraic in each time step, obtaining the values of the displacements $\overline{\boldsymbol{u}}_{n+1}^{global}$ and pore water pressure $\overline{\boldsymbol{p}}_{wn+1}^{global}$ at time t_{n+1} by the difference equations (13) and(14).

4 VALIDATION

The large scale model test conducted in 2004 by Kudella and Oumeraci (Kudella et al 2006) in the Large Wave Flume (GWK) of Hannover is numerically reproduced under the scope of the soil-water-structure interaction model proposed in the present paper.

The cross section of the large scale model test model, including the position of the transducers used at the caisson and its foundation are shown in Figure 3. The sand beneath the caisson was selected as fine as practicably feasible with D_{50}=0.21mm, D_{10}=0.13mm y D_{60}/D_{10}=1.69. The initial relative density, was estimated to vary between D_r=0.15 and D_r=0.33. The sand beneath the caisson was rinsed to achieve the highest practicably feasible saturation value.

The seaward berm consists of a 35cm thick armor layer, a 20cm filter layer and a 45cm core. The caisson is placed on a 20cm thick rubble layer.

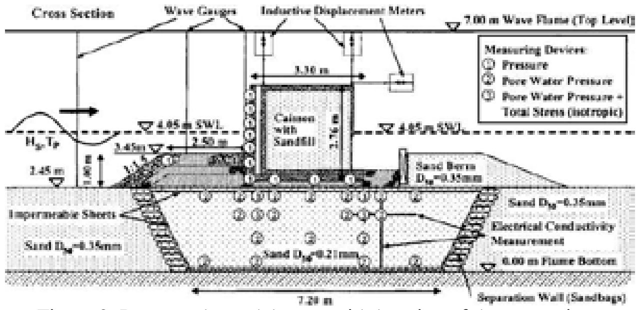

Figure 3. Large scale model setup with location of the measuring device, after Kudella 2006.

Considering the model setup, the test program performed by Kudella and Oumeraci was able to obtain breaking wave impact loads.

The model proposed in the present paper has been able to reproduce adequately the principal characteristics of the caisson oscillations and instantaneous pore pressure generation experimentally deduced under breaking wave impact loads (Figure 4, Figure 5).

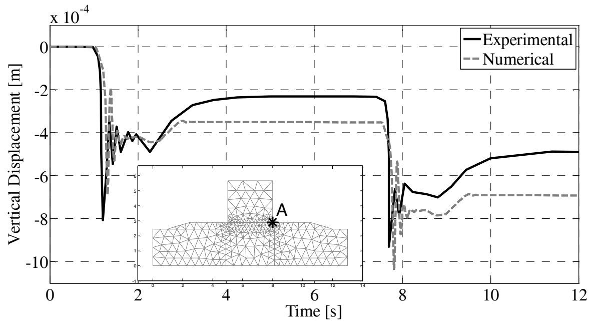

Figure 4. Numerical and experimental vertical displacement at shoreward caisson edge induced by two impulsive sea wave actions *(H=0.6m, T=6.5s, h_s=1.6m, h_1=0.6m).*

In Figure 4 and 5 is possible to observe that under impulsive wave actions, define by the height wave (*H*), the wave period (*T*), the water deep at toe of the structure (h_s) and the water deep over seaward berm (h_1), the excess pore pressure trace follows closely the caisson vertical displacement. There is no excess pore pressure variation until the movement of the caisson starts. As the rear edge of the caisson moves downwards, the soil layer compacts inducing a positive excess pore pressure. The pore pressure increase ends at the same time as the shoreward edge of the caisson begins to move upwards. The caisson oscillation experimented after the peak vertical displacement is accurately followed by an excess pore pressure oscillation. After this oscillations, the rear edge of the caisson returns partially to its original position with a correlated decrease in excess pore pressure.

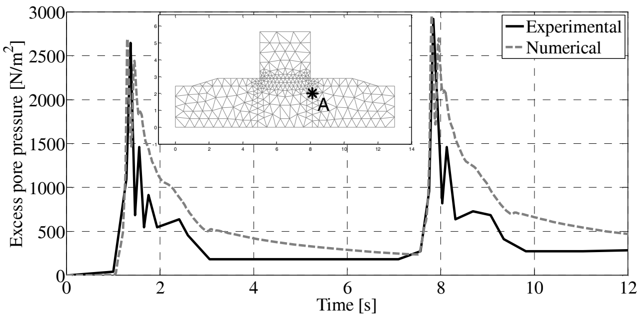

Figure 5. Numerical and experimental excess pore pressure obtain under the shoreward caisson edge induced by two impulsive wave actions ($H=0.6m$, $T=6.5s$, $h_s=1.6m$, $h_1=0.6m$).

The proposed model is also able to reproduce satisfactorily the accumulative settlement behaviour of a vertical breakwater structure subjected to series of sea wave impacts, eventually leading to a diffuse failure mechanism. It is also able to simulate adequately the correlation between accumulated settlements and residual pore pressure (Figure 6).

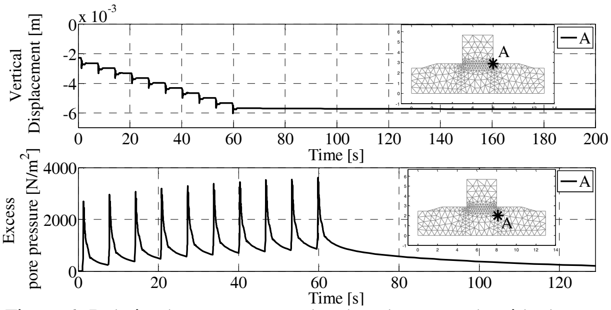

Figure 6. Relation between accumulated settlement and residual pore pressure ($H=0.6m$, $T=6.5s$, $h_s=1.6m$, $h_1=0.6m$). Numerical result

The relation shown in Figure 6 indicates a residual pore pressure directly induced by the impulsive action derived caisson motion. The partial drainage performed between two wave impact loads is not enough to dissipate the entire excess pore pressure generated therefore a pore pressure accumulation process is developed. Just before a tenth impact load takes place, the accumulated excess pore pressure close to the sand layer surface is almost $0.8\,kN/m^2$. Once the impulsive wave action is finished, no extra excess pore pressure generation is performed but a pure dissipation process develops. While this dissipation process is taking place, the extra settlements observed induced by an elastoplastic consolidation process are negligible. After $200s$ the pore pressure derived by impulsive wave action dissipates completely in the vicinity of the sand layer surface.

5 CONCLUSIONS

A theoretical model for the soil-water-structure interaction that permits the analysis of non-linear seafloor dynamics induced by sea wave actions in a vertical breakwater structure is presented.

Proposed model is able to analyze the fundamental aspects involved in the geomechanics associated with the foundation of gravity maritime structures: Complex caisson-rubble mound interaction, soil skeleton-pore fluid coupling and degradation of the seabed and long term effects mainly due to repetitive loading, eventually leading to a diffuse failure mechanism.

The principal characteristics of the instantaneous response experimentally deduced are reproduced adequately. Moreover, the model proposed is able to reproduce satisfactorily the accumulative settlement behaviour induced by impulsive sea wave actions including correlation with pore pressure increase and effective stress decrease.

6 REFERENCES

Goda Y. 1994. Dynamic Response of Upright Breakwaters to Impulsive Breaking Wave Forces. *Coastal Engineering*, 22(1-2). 135-158.

Jeng D.S., Cha D.H., Lin Y.S. 2001. Wave-Induced Pore Pressure Around a Composite Breakwater. *Ocean Eng*., 28(10), 1413-1435.

Jeng D.S. and Cha D.H. 2003. Effects of Dynamic Soil Behavior and Wave Non-Linearity on the Wave-Induced Pore Pressure and Effective Stresses in Porous Seabed. *Ocean Eng*. 30(16), 2065-2089.

Kudella M., Oumeraci H., De Groot M.B. 2006. Large-Scale Experiments on Pore Pressure Generation Underneath a Caisson Breakwater. *J. Waterw. Port. Coastal Ocean Div. Am. Soc. Civ. Eng*. 132(4), 310-324.

Mira P., Tonni L., Pastor M. 2009. A Generalized Midpoint Algorithm for the Integration of a Generalized Plasticity Model for Sands. *Int. J. Numer. Methods Eng*., 77(9). 1201-1223.

Oumeraci H. and Kortenhaus A. (1994). Analysis of the Dynamic Response of Caisson Breakwaters. *Coastal Engineering*, 22. 159-183.

Pastor M., Drempetic V., Merodo J.A.F. (2006). Una Metodología Racional Para El Estudio De Cimentaciones De Estructuras Marinas. *Ingeniería Civil. CEDEX*., 141. 37-48.

Sloan W. and Randolph M.F. 1982. Numerical Prediction of Collapse Loads using Finite Element Methods. *Int. J. Numer. Analyt. Meth. Geomech*., 6(1). 47-76.

Stickle M.M. 2010. *Sobre La Respuesta Dinámica Del Terreno Bajo La Acción Del Olaje En Cajones Fondeados En Suelos Arcillosos*. PhD Tesis, Universidad Politécnica de Madrid.

Ulker M.B.C., Rahman M.S. and Guddati M.N. 2010. Wave-Induced Dynamic Response and Instability of Seabed Around Breakwater. *Ocean Engineering*, 37. 1522-1545

Yamamoto T., Koning H.L. and Sellmejjer H. 1978. On the Response of a Poro-Elastic Bed to Water Waves. *J. Fluid Mech*., 87. 193-206.

Zienkiewicz O.C. and Shiomi T. 1984. Dynamic Behavior of Saturated Porous Media: The Generalized Biot Formulation and its Numerical Solution. *Int. J. Numer. Analyt. Meth. Geomech*., 8. 71-96.

Zienkiewicz O.C., Chan A.H.C., Pastor M. 1999. *Computational Geomechanics. With Special Reference to Earthquake Engineering.* JOHN WILEY & SONS.